

# A RECURSIVE MODEL FOR LASER-ELECTRON-RADIATION INTERACTION IN INSERTION SECTION OF SSMB STORAGE RINGS BASED ON THE TRANSVERSE-LONGITUDINAL COUPLING SCHEME

Cheng-Ying Tsai\*, Huazhong University of Science and Technology, Wuhan, China  
 Xiujie Deng, Tsinghua University, Beijing, China

## Abstract

Recently, a mechanism of steady-state microbunching (SSMB) in the storage ring has been proposed and investigated. The SSMB aims to maintain the same excellent high repetition rate, close to continuous-wave operation, as the storage ring. Moreover, replacing the conventional RF cavity with a laser modulator for longitudinal focusing, the individual electron bunches can be microbunched in a steady state. The microbunched electron bunch train, with an individual bunch length comparable to or shorter than the radiation wavelength, can not only produce coherent powerful synchrotron radiation but may also be subject to FEL-like collective instabilities. Our previous analysis was based on the wake-impedance model. In this paper, we have developed a recursive model for the laser modulator in the SSMB storage ring. In particular, the transverse-longitudinal coupling scheme is assumed. Equipped with the matrix formalism, we can construct a recursive model to account for turn-by-turn evolution, including single-particle and second moments. It is possible to obtain a simplified analytical expression to identify the stability regime or tolerance range for non-perfect cancellation.

## INTRODUCTION

Recently there has been a growing interest in the mechanism of the so-called steady-state microbunching (SSMB) in a storage ring proposed as a potential new light source [1–5]. The existing literature for the studies of electron dynamics in the laser modulators mainly focuses on single-particle dynamics, e.g., Refs. [6–9], or the radiation output characteristics based on the prescribed electron trajectories [10, 11]. The collective dynamics occurring in the laser modulators has only recently been studied [12–14] using the wake-impedance model for the case of a *single* laser modulator.

In a current design a pair of two laser modulators, where the radiator is sandwiched, is considered; see Fig. 1. In this work we propose an alternative model to study the laser-electron-radiation interaction in the laser modulators of SSMB storage rings based on the transverse-longitudinal coupling (TLC) scheme [10], by constructing a recursive model to account for multi-pass radiation dynamics in nonlinear regime to analyze multi-bunch multi-turn dynamics [9]. In the model there are two options for us to study the dynamics: non-perfect kick model and FEL-like model.

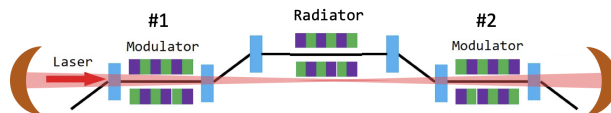


Figure 1: Conceptual schematic layout of SSMB laser modulator based on TLC scheme. The two laser modulators can be independent.

## THEORETICAL FORMULATION

In the recursive formulation, the laser-electron-radiation dynamics can in principle be nonlinear. However the energy chirp is linearized; therefore the validity is limited to  $\sigma_z \ll \lambda_L$ . We assume the microbunch circulates clockwise. Considering the state vector  $[y \ y' \ z \ \delta]^T$  at the middle of the storage ring (e.g., at RF or main-ring laser modulator), the transport from which to the insertion entrance can be formulated as a half ring  $\mathbf{R}_{1/2}$ , which is

$$\begin{pmatrix} \cos \pi \nu_y & \beta_y \sin \pi \nu_y & 0 & 0 \\ -\frac{1}{\beta_y} \sin \pi \nu_y & \cos \pi \nu_y & 0 & 0 \\ 0 & 0 & \cos \pi \nu_s & \beta_z \sin \pi \nu_s \\ 0 & 0 & -\frac{1}{\beta_z} \sin \pi \nu_s & \cos \pi \nu_s \end{pmatrix}, \quad (1)$$

where  $\beta_y, \nu_y$  and  $\beta_z, \nu_s$  parametrize the transverse and longitudinal motions, respectively. The synchrotron tune  $\nu_s$  is determined by the RF/laser modulator of the storage ring with the slippage factor  $\eta_{\text{ring}}$  and the circumference  $C_{\text{ring}}$ . Here we have implicitly assumed Courant-Snyder functions are the same at the RF, the entrance and exit of the insertion section. The insertion section begins from the vertical bending magnet

$$\mathbf{M}_B = \begin{pmatrix} 1 & 0 & 0 & 0 \\ 0 & 1 & 0 & R_{46} \\ -R_{46} & 0 & 1 & 0 \\ 0 & 0 & 0 & 1 \end{pmatrix}, \quad (2)$$

and the following first laser modulator

$$\mathbf{M}_{LM}^{(1)} = \begin{pmatrix} 1 & N_u \lambda_u & 0 & 0 \\ 0 & 1 & 0 & 0 \\ 0 & 0 & \cos \chi^{(1)} & \frac{R_{56,LM}}{\chi^{(1)}} \sin \chi^{(1)} \\ 0 & 0 & \frac{h^{(1)}}{\chi^{(1)}} \sin \chi^{(1)} & \cos \chi^{(1)} \end{pmatrix}, \quad (3)$$

with  $N_u, \lambda_u$  the number and period length of the undulator,  $\chi^{(1)} = \sqrt{-R_{56,LM} h^{(1)}}$ ,  $R_{56,LM}, h$  being the longitudinal

\* jcytsai@hust.edu.cn

dispersion and the imposed chirp strength. The second laser modulator shall be denoted by the superscript (2). Before entering the radiator, a dogleg is used to compress the beam

$$\mathbf{M}_{DL} = \begin{pmatrix} 1 & 0 & 0 & R_{54} \\ 0 & 1 & 0 & 0 \\ 0 & R_{54} & 1 & R_{56} \\ 0 & 0 & 0 & 1 \end{pmatrix}. \quad (4)$$

The above three elements are combined to be the first half of the insertion section  $\mathcal{T}_{1/2}^{(1)} = \mathbf{M}_{DL}\mathbf{M}_{LM}^{(1)}\mathbf{M}_B$ . TLC scheme requires the matrix elements to satisfy [10]

$$\begin{aligned} R_{56}h + 1 &= 0, \\ R_{56} + R_{54}R_{46} &= 0. \end{aligned} \quad (5)$$

In the non-perfect kick model we will relax the first condition, considering non-perfect cancellation of the two laser modulators. The one-turn map can be constructed  $O = \mathbf{R}_{1/2}\mathcal{T}_{1/2}^{(2)}\mathcal{T}_{1/2}^{(1)}\mathbf{R}_{1/2}$  around the main-ring RF, with the  $\mathcal{T}_{1/2}^{(2)}$  being the reverse order of the  $\mathcal{T}_{1/2}^{(1)}$ . Ideally,  $\mathcal{T}_{1/2}^{(2)}\mathcal{T}_{1/2}^{(1)} = I$  being the identity map. When considering the radiation dynamics in the laser modulators, the above  $\mathbf{M}_{LM}^{(1,2)}$  may vary turn after turn and the one-turn map perturbed, i.e.,  $O \rightarrow O_n$ . The microbunch centroid evolves based on  $X_{n+1} = OX_n$ . The beam second moments evolve according to  $\Sigma_{n+1} = O\Sigma_n O^T$ . The bunching factor of the microbunch train is estimated as  $|b_n| = e^{-\frac{1}{2}\left(\frac{2\pi}{\lambda_L}\right)^2 \sigma_{z,n}^2}$  where  $\sigma_{z,n}$  can be obtained from beam sigma matrix  $\Sigma_n$ . Here we assume identical microbunches in the bunch train.

### Non-perfect Kick Model

This is not a dynamical model but can be used to investigate to what extent the non-perfect cancellation of two laser modulators may lead to unstable operation. Here the imperfect kick is added according to  $h^{(2)} \rightarrow h^{(1)}(1 + \varepsilon)$  with  $\varepsilon$  the deviation from the idealized, symmetric situation  $h^{(2)} = h^{(1)}$ . The first laser modulator is assumed perfect.

### FEL-like Model

The turn-by-turn dependence of  $\mathbf{M}_{LM}^{(1,2)}$  originates from the variation of chirp strength  $h_n^{(1,2)}$ . More specifically [15],

$$h_n^{(1,2)} = \frac{e[JJ]K}{\gamma^2 mc^2} \sqrt{\frac{4P_{L,n}^{(1,2)} Z_0 Z_R}{\lambda_L}} \tan^{-1} \left( \frac{L_u}{2Z_R} \right) k_L. \quad (6)$$

The turn-by-turn evolution of the laser power in the two laser modulators  $P_{L,n}^{(1,2)}$ , perturbed by the radiating microbunches, can be formulated using a simplified FEL model. Skipping the details, the  $n$ th-turn laser power can be evaluated as

$$P_{L,n}^{(1,2)} = P_{L,n}^{\text{ext}} + \frac{g_0}{4N_u} |b_n^{(1,2)}|^2 P_{\text{beam}}, \quad (7)$$

where  $P_{L,n}^{\text{ext}}$  is the external laser,  $g_0$  is the small-signal gain. The laser power evolves from  $n$ -th turn to  $(n+1)$ -th turn as

$$P_{L,n+1} = R(1 + G_n)P_{L,n}, \quad (8)$$

with  $R$  the total mirror reflection loss and the gain per pass  $G_n = G_{M,n} \frac{1 - e^{-\beta X_n}}{\beta X_n}$  with  $\beta = \frac{\pi}{2}(1.0145)$ ,  $X_n = \frac{P_{L,n}}{P_{\text{sat}}}$ ,  $P_{\text{sat}} \left( \frac{\text{MW}}{\text{cm}^2} \right) = 6.93 \times 10^2 \left( \frac{\gamma}{N_u} \right)^4 \frac{1}{(\lambda_u(\text{cm})K[JJ])^2}$  and  $G_{M,n}$  can be parameterized by [16]

$$G_{M,n} = \frac{e^{-0.132P(g_0)\mu_{\epsilon,n}^2}}{1 + 1.6Q(g_0)\mu_{\epsilon,n}^2} \sum_{s=1}^3 g_0^s g_s(\kappa), \quad (9)$$

with the normalized energy spread and detuning parameter  $\mu_{\epsilon} = 4N_u\sigma_{\delta,n}$ ,  $\kappa = 2\pi N_u \frac{\omega_L - \omega}{\omega_L}$ .

## SIMULATION RESULTS

In the following simulations we assume  $\beta_y \approx 10$  m at the entrance of first modulator undulator with  $\nu_y \sim C_{\text{ring}}/2\pi\beta_y$ . We further assume that the bunch length and energy spread are 500 nm and  $3 \times 10^{-4}$  around the storage ring (outside the insertion section). The  $R_{46}$  is estimated as  $R_{46} \approx \sqrt{\frac{\mathcal{H}_y(\text{Mod})}{\beta_y}}$  with  $\mathcal{H}_y(\text{Mod}) \approx \frac{\sigma_z^2(\text{Mod})}{\epsilon_y^G}$  [10]. Then according to Eq. (5), the remaining matrix elements can be determined in order

$$R_{56} = -\frac{1}{h}, \quad R_{54} = -\frac{R_{56}}{R_{46}}, \quad (10)$$

for the doglegs associated with two laser modulators. Other relevant beam parameters are: beam energy 360 MeV, average bunch current 1 A, vertical emittance  $\epsilon_y^G = 10$  pm. The storage ring parameters:  $C_{\text{ring}} = 50$  m and  $\eta_{\text{ring}} = 10^{-6}$ . The nominal laser modulator parameters:  $\lambda_L = 1 \mu\text{m}$ ,  $K_u = 3.35$ ,  $\lambda_u = 15$  cm,  $N_u = 13$ , and the total mirror reflectivity  $R \approx 0.99963$ . The bunch length at the radiator is for the moment assumed to be 20 nm [17]. The radiation wavelength at the radiator is targeted as 200 nm.

### Results Based on Non-perfect Kick Model

Figures 2 summarizes the simulation results. By scanning a range of  $\varepsilon$ , we find that the beam is stable in the range of  $-0.012 \leq \varepsilon \leq 0.045$ . Outside the region the beam becomes unstable; the microbunch length becomes larger than the laser modulation wavelength and the radiation power at radiator exhibits large oscillation. For the perfect-cancellation case of  $\varepsilon = 0$ , the bunch length remains a constant, approximately 21.3 nm. For the case with  $\varepsilon \neq 0$ , the bunch length disperses and becomes larger when  $|\varepsilon|$  increases. This model assumes  $R = 1$ , i.e., no reflectivity loss.

### Results Based on FEL-like Model

For simplicity, assume no initial detuning, i.e.,  $\kappa = 0$ , of the two modulator undulators. On the first few turns we expect the results to be close to that of perfect-kick model  $\varepsilon = 0$ . The FEL-like model accounts for the mirror reflectivity loss. In the simulation case, for the initial laser modulation power  $P_L^{(1,2)} \approx 274$  kW, meaning that we have 101 W due to the reflectivity loss. Let us assume the external injection of modulation laser power is 100 W per pass to compensate

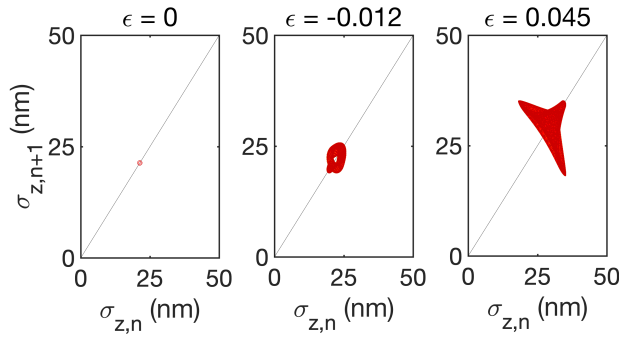


Figure 2: Turn-by-turn evolution of bunch length at the radiator for three cases.  $\sigma_z \approx 21.3$  nm for perfect cancellation.

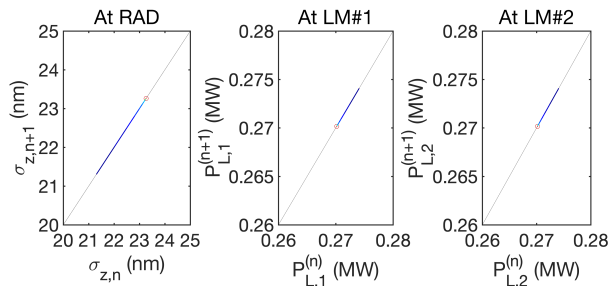


Figure 3: Turn-by-turn evolution of the bunch length and the stored radiation power in the two laser modulators. The evolution begins from blue and gradually evolve to red.

the loss. Figure 3 shows the turn-by-turn microbunch length at radiator, the laser power stored in the two modulators.

Figure 4 displays turn-by-turn evolution of the microbunch length, vertical beam size at the radiator and at the entrance of the first modulator based on the perfect-kick model and FEL-like model. At the very beginning the two models give the same prediction, as expected. As time goes by, they deviate, particularly for the microbunch length. The microbunch lengthening at the radiator is due to gradual decrease of longitudinal focusing strength, resulting from transient imbalance from cavity reflection loss, the injection compensation, and the FEL-like gain per pass. After about  $2 \times 10^4$  turns the system reaches a steady state. Note that here we assume no initial detuning of the two modulator undulators. A proper detuning, together with knowledge of laser cavity design, may help retain the microbunch length at its design value at the radiator.

Figure 5 illustrates the output power at the radiator and the corresponding bunching factor based on the two models. The radiation power is targeted at 200 nm, where the microbunch length is about 20 nm in design. The slight microbunch lengthening leads to bunching factor degradation and decrease of the output power.

## SUMMARY AND DISCUSSION

For perfect cancellation of the two laser modulators, the developed matrix formulation gives consistent results with the analytical estimate [17]. There are two options to con-

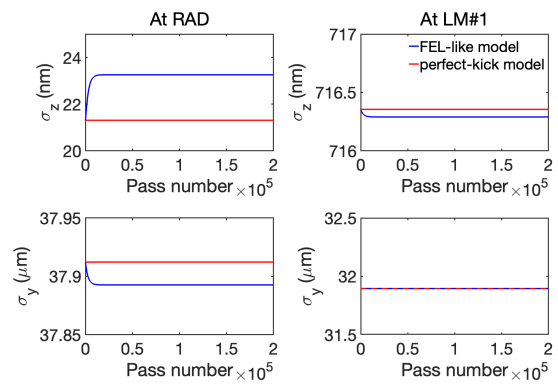


Figure 4: Turn-by-turn evolution of the microbunch length, vertical beam size at the radiator (left) and at the entrance of the first modulator (right) based on the perfect-kick model (red) and FEL-like model (blue).

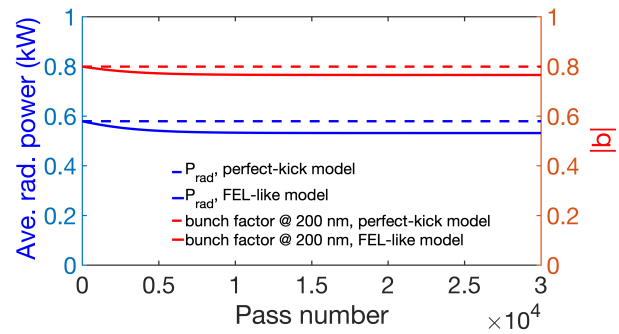


Figure 5: Output radiation power at the radiator and the corresponding bunching factor based on the perfect-kick model (dashed line) and FEL-like model (solid line).

sider the effects of laser modulators on the beam. One is by adding a static (same for each turn) deviation parameter  $\epsilon$  to the chirp strength at the second modulator to account for non-perfect cancellation. The other is by evaluating the turn-by-turn radiation power evolution stored in the two laser modulators based on FEL-like model. Comparing the FEL-like model with non-perfect static kick model, we find that

- Variation of microbunch length at radiator becomes larger, when using both the non-perfect kick model and the FEL-like model, see Figs. 2 and 4;
- The static and stable operation may require the chirp strength deviation within  $-0.012 \leq \epsilon \leq 0.045$ , where  $h_n^{(2)} = h_n^{(1)}(1 + \epsilon)$ ;
- The imbalance and/or gradual decrease of longitudinal focusing strength, i.e., chirp strength  $h_n^{(1,2)}$ , due to cavity loss can be compensated by a proper detuning and/or re-injection of the external modulation laser power.

We have constructed a recursive model to account for turn-by-turn evolution, including beam centroid and moment stability. It is possible to obtain a simplified analytical expression to identify the stability regime or tolerance range for non-perfect cancellation. This work is ongoing.

## ACKNOWLEDGMENTS

The authors are grateful for many insightful comments from Prof. A.W. Chao. This work is supported by the Fundamental Research Funds for the Central Universities (HUST) under Project No. 2021GCRC006 and National Natural Science Foundation of China under project No. 12275094.

## REFERENCES

- [1] D. F. Ratner and A. W. Chao, “Steady-state microbunching in a storage ring for generating coherent radiation” *Phys. Rev. Lett.* vol. 105, p. 154801, 2010.  
doi:10.1103/PhysRevLett.105.154801
- [2] A. W. Chao *et al.*, “High power radiation sources using the steady-state microbunching mechanism”, in *Proc. 7th Int. Particle Accelerator Conf. (IPAC’16)*, Busan, Korea, Jun. 2016, paper TUXB01, pp. 1048-1053.  
doi:10.18429/JACoW-IPAC2016-TUXB01
- [3] C. Tang *et al.*, “An overview of the progress on SSMB”, in *Proc. 60th ICFA Advanced Beam Dynamics Workshop on Future Light Sources (FLS 2018)*, Shanghai, China, March 2018, paper THP2WB02, pp. 166-170.  
doi:10.18429/JACoW-FLS2018-THP2WB02
- [4] X. Deng *et al.*, “Experimental demonstration of the mechanism of steady-state microbunching”, *Nature*, vol. 590, no. 7847, pp. 576-579, 2021.  
doi:10.1038/s41586-021-03203-0
- [5] A.W. Chao, “Storage ring based steady state microbunching”, presented at FLS’23, Lucerne, Switzerland, Aug 2023, paper MO2L2, this conference.
- [6] Y. Zhang *et al.*, “Ultralow longitudinal emittance storage rings”, *Phys. Rev. Accel. Beams*, vol 24, pp. 090701, 2021.  
doi:10.1103/PhysRevAccelBeams.24.090701
- [7] Z. Pan *et al.*, “A Storage Ring Design for Steady-State Microbunching to Generate Coherent EUV Light Source”, in *Proc. 39th Int. Free-Electron Laser Conf. (FEL’19)*, Hamburg, Germany, Aug. 2019, paper THP055, pp. 700-703.  
doi:10.18429/JACoW-FEL2019-THP055
- [8] X. J. Deng *et al.*, “Single-particle dynamics of microbunching”, *Phys. Rev. Accel. Beams*, vol. 23, pp. 044002, 2020.  
doi:10.1103/PhysRevAccelBeams.23.044002
- [9] Z. Li *et al.*, “Generalized longitudinal strong focusing in a steady-state microbunching storage ring”. submitted for publication.
- [10] X. J. Deng *et al.*, “Harmonic generation and bunch compression based on transverse-longitudinal coupling”, *Nucl. Instrum. Methods Phys. Res. Sect. A*, vol. 1019 p. 165859, 2021. doi:10.1016/j.nima.2021.165859
- [11] X. J. Deng *et al.*, “Average and statistical properties of coherent radiation from steady-state microbunching”, *J. Synchrotron Radiat.*, vol. 30, pp. 35-50, 2023.  
doi:10.1107/S1600577522009973
- [12] C.-Y. Tsai *et al.*, “Coherent-radiation-induced longitudinal single-pass beam breakup instability of a steady-state microbunch train in an undulator”, *Phys. Rev. Accel. Beams*, vol. 24, p. 114401, 2021.  
doi:10.1103/PhysRevAccelBeams.24.114401
- [13] C.-Y. Tsai, “Theoretical formulation of multiturn collective dynamics in a laser cavity modulator with comparison to robinson and high-gain free-electron laser instability”, *Phys. Rev. Accel. Beams*, vol. 25, p. 064401, 2022.  
doi:10.1103/PhysRevAccelBeams.25.064401
- [14] C.-Y. Tsai, “Longitudinal single-bunch instabilities driven by coherent undulator radiation in the cavity modulator of a steady-state microbunching storage ring”, *Nucl. Instrum. Methods Phys. Res. Sect. A*, vol. 1042, p. 167454, 2022.  
doi:10.1016/j.nima.2022.167454
- [15] A. W. Chao, “Focused laser”, unpublished.
- [16] G. Dattoli *et al.*, “Booklet for FEL design: a collection of practical formulae”. [https://fel.enea.it/booklet/pdf/Booklet\\_for\\_FEL\\_design.pdf](https://fel.enea.it/booklet/pdf/Booklet_for_FEL_design.pdf)
- [17] X. J. Deng, “10  $\mu\text{m}$  and 1  $\mu\text{m}$  SSMB”, unpublished.